Aqueous injection of quercetin: an approach for confirmation of its direct in vivo cardiovascular effects

***Graphical Abstract (for review)**

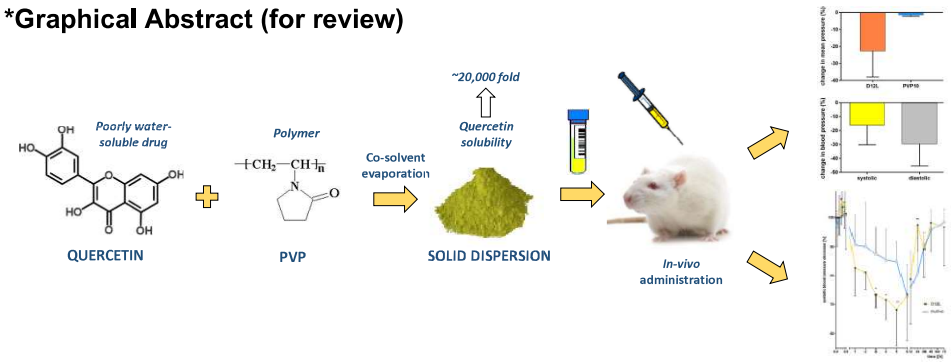

Aqueous injection of quercetin: an approach for confirmation of its direct *in vivo* cardiovascular effects

Elena Piera Porcu[a], *Massimo Cossu*[a], *Giovanna Rassu*[a], *Paolo Giunchedi*[a], *Guido Cerri*[b], *Jana Pourová*[c], *Iveta Najmanová*[d], *Thomas Migkos*[c], *Veronika Pilařová*[e], *Lucie Nováková*[e], *Přemysl Mladěnka*[c]*, *Elisabetta Gavini*[a]*

Affiliations:

[a]Department of Chemistry and Pharmacy, University of Sassari, Sassari, Italy

[b]Department of Architecture, Design and Urban Planning - GeoMaterials Lab, University of Sassari, Sassari, Italy

[c]Department of Pharmacology and Toxicology, Faculty of Pharmacy in Hradec Králové, Charles University, Czech Republic

[d]Department of Biological and Medical Sciences, Faculty of Pharmacy in Hradec Králové, Charles University, Czech Republic

[e]Department of Analytical Chemistry, Faculty of Pharmacy in Hradec Králové, Charles University, Czech Republic

E-mail address:

Elena Piera Porcu: elena.piera1988@gmail.com

Massimo Cossu: mcossu@uniss.it

Giovanna Rassu: grassu@uniss.it

Paolo Giunchedi: pgiunc@uniss.it

Guido Cerri: gcerri@uniss.it

Jana Pourová: pourova@faf.cuni.cz

Iveta Najmanová: najmanoi@faf.cuni.cz

Thomas Migkos: migkost@faf.cuni.cz

Veronika Pilařová: pilarovv@faf.cuni.cz

Lucie Nováková: novakoval@faf.cuni.cz

Přemysl Mladěnka: mladenkap@faf.cuni.cz

Elisabetta Gavini: eligav@uniss.it

Corresponding Authors

*Prof. Elisabetta Gavini, Department of Chemistry and Pharmacy University of Sassari, via Muroni 23/a, 07100 Sassari, Italy Tel: +39079228752; E-mail address: eligav@uniss.it

*Assoc. Prof. Přemysl Mladěnka, Department of Pharmacology and Toxicology, Faculty of Pharmacy, Charles University, Akademika Heyrovského 1203, 500 05 Hradec Králové, Czech Republic, Tel: +420495067295; E-mail address: mladenkap@faf.cuni.cz

Authors contribution:

Elena Piera Porcu, Massimo Cossu and Giovanna Rassu: carried out the experimental pharmaceutical work;

Paolo Giunchedi contributed to the interpretation of the results;

Guido Cerri performed the physical-chemical studies;

Jana Pourová, Iveta Najmanová and Thomas Migkos performed the *in vivo* study;

Veronika Pilařová and Lucie Nováková carried out pharmacokinetic analysis of blood samples;

Přemysl Mladěnka designed the *in vivo* experiments, critically analysed the data and wrote corresponding parts of the article;

Elisabetta Gavini provided the intellectual input and designs and approved the protocols to be followed in the study and wrote the article.

All authors discussed the results and contributed to the final manuscript.

ABSTRACT

Potential positive effects of flavonol quercetin on humans were suggested by many studies. However, it is not clear if these effects are mediated by quercetin or its metabolites. The *in vivo* confirmation of quercetin effects is largely hindered by its low water solubility and thus impossibility to test directly its impact. Therefore, a solid dispersion of quercetin with polyvinylpyrrolidone (PVP) was developed to prepare an injectable formulation of water-soluble quercetin. The optimized formulation provided a 20,000-fold increase in quercetin solubility. This formulation was tested on conventional and spontaneously hypertensive rats; it lowered their blood pressure in both short- and long-term basis. Pharmacokinetic data are also provided. This study reports for the first time an injectable water-soluble formulation of quercetin suitable for confirmation of its vascular effect *in vivo*.

Keywords: Solid dispersion; Cardiovascular effects; Quercetin; Polyvinylpyrrolidone; Solubility enhancement; Injectable aqueous solution.

1. INTRODUCTION

Flavonoids always attracted a great attention due to their presence in common diet and their possible positive effects on humans (Kumar and Pandey, 2013; Mladěnka et al., 2010). The major flavonol in the human diet is quercetin and indeed, most flavonoid studies have been performed with it. There is a huge number of studies showing its positive effects, and in particular, some are claiming lowering arterial blood pressure (Larson et al., 2010). However, notwithstanding such enormous quantity of articles, there are still no definite proofs if quercetin has clearly positive effects on human being. The major controversies arise from the facts that orally given quercetin has very low bioavailability (Li et al., 2009; Rothwell et al., 2016), and its *in vitro* effects were commonly observed in quite large concentrations which are hardly, if at all, achievable after oral intake. Another possible explanation is based on the fact that although quercetin is poorly absorbed, it is extensively metabolized by human microflora into a number of small phenolic compounds which can have significant biological effects in humans (Del Rio et al., 2013). For example, our group recently demonstrated than at least one of these metabolites lowers arterial blood pressure in rat (Najmanová et al., 2016). In order to confirm or refute the direct effect of quercetin on arterial blood pressure, a water-soluble formulation of quercetin is needed since only biologically friendly solvents are fully compatible with biological systems and can be applied intravenously without producing inadvertent additional effects.

In general, the use of quercetin in pharmaceutical area is still limited due to its poor solubility in water, which limits formulation strategies. Because of scarce hydrophilicity, quercetin shows low dissolution rate, and consequently minimal quercetin absorption occurs in the gastrointestinal tract (Li et al., 2009; Puerta et al., 2017). For this reason, several efforts have been made to improve the aqueous solubility and therapeutic effects of quercetin.

Various approaches such as polymeric nanoparticles (Wang et al., 2016), cocrystals (Smith et al., 2011), lipid nanoparticles (Bose et al., 2013; Li et al., 2009; Kumar et al., 2016), complexation (Jullian

et al., 2007; Sri et al., 2007), micelles (Gao et al., 2012), emulsions (Gao et al., 2009; Tran et al., 2014; Hädrich et al., 2016), liposomes (Caddeo et al., 2016) and solid dispersion have been developed to enhance the solubility, dissolution rate and bioavailability of quercetin. Solid dispersions refer to a solid product made up of at least two different components, generally a hydrophilic and inert matrix and one or more hydrophobic drugs. In these systems, the drug solubility and its dissolution profile can be improved through the amorphous solid state and by reducing the particle size of the drug. Additionally, the use of hydrophilic carriers increases the wettability of hydrophobic drugs (Park et al., 2016). In particular, various polymers have been employed to increase quercetin solubility such as polyethylene glycols (PEGs) (Otto et al., 2013; Park et al., 2016), cellulose derivatives (Sansone et al., 2011; Li B. et al., 2013; Gilley et al., 2017) and polyvinylpyrrolidone (Povidone, PVP) (de Mello Costa et al., 2010; Kakran et al., 2011; Yan et al., 2014).

PVP is one of the most commonly used carriers for solid dispersions due to its amphiphilic properties, nontoxicity and biocompatibility. Indeed, PVP is known to form water-soluble complexes with several drugs including carbamazepine (Sethia and Squillante, 2004), lansoprazole (Zhang et al., 2008), efavirenz (Alves et al., 2014), atorvastatin (Jahangiri et al., 2015) and others. In all cases, the aqueous solubility of the product is largely improved.

PVP is available in different grades based on molecular weights (Kadajji and Betageri, 2011). The mean molecular weight of PVP is characterized by the K-value (e.g. Povidone K-12, Povidone K-17, Povidone K-25, Povidone K-30, Povidone K-90) (Folttmann and Quadir, 2008). PVPs with low K-value are suitable solubilizing agents particularly for injectables (e.g. rifampicin, sulfonamide, melphalan, metronidazole, trimethoprim formulations) due to their low viscosity.

The solid dispersions represent a profitable strategy because of its simplicity and efficacy for enhancing the solubility and bioavailability of poorly soluble drugs. This aspect has led to an increase in their applications in the area of cosmetics and pharmaceuticals. Solid dispersions can be prepared by

129 different techniques (Vasconcelos et al., 2007; Sareen et al., 2012). Solvent evaporation method is
130 particularly suitable for PVPs due to their good solubility in most solvents. In addition, co-solvent
131 technique is particularly important for parenteral dosage forms. Due to this method, it is possible to
132 incorporate a large quantity of a drug in small volume of liquid, as required for injections (Soni et al.,
133 2014).
134 Although there are many papers in the literature regarding the formulation improving delivery and
135 solubility of quercetin in different delivery systems, very few studies have investigated the possibility
136 of preparing quercetin formulations for injection (Yuan et al., 2006; Date et al., 2008; Sun et al., 2011);
137 particularly scarce is the literature concerning the development of injectable aqueous solutions. These
138 systems may be of significant utility not only for a possible therapeutic application but also for
139 studying the real direct effects of quercetin *in vivo,* through a simple system enabling easy dose
140 modification. For these reasons, the objective of the present work was to prepare an aqueous
141 formulation of quercetin for i.v. injection to evaluate its antihypertensive effects *in vivo*. For this
142 purpose, a solid dispersion powder of quercetin with PVP suitable for injections was developed by
143 using the co-solvent method.

144

145 **2. MATERIALS AND METHODS**

146

147 **2.1 Materials**

148 Quercetin (purity ≥ 95%) and polyvinylpyrrolidone (PVP10, Mw=10000 g/mol, K-value 13-19) were
149 purchased from Sigma Aldrich (Milan, Italy). Saline (0.9 % NaCl injectable solution) was supplied by
150 Eurospital (Trieste, Italy). Ethanol 96 % was purchased from Carlo Erba Reagents (Italy). Analytical
151 grade solvents were used.

152

2.2 Preparation of solid dispersions

Solid dispersions of quercetin with the different weight ratios of quercetin/PVP10 were obtained by using the co-solvent evaporation technique. Briefly, the solutions were prepared by dissolving 25 mg of quercetin in 12.5 ml of ethanol and variable amounts of PVP10 in 40 ml of deionized water (Table 1).

Table 1. Qualitative and quantitative composition of all formulations.

FORMULATION	QUERCETIN (mg)	PVP10 (mg)	Weight Ratio QUERCETIN/ PVP10 (w/w)	Theoretical Drug Content QUERCETIN (%)
D3L	25	62.5	1/2.5	28.5
D5L	25	125	1/5	16.7
D10L	25	250	1/10	9.1
D11L	25	275	1/11	8.3
D12L	25	300	1/12	7.7
D15L	25	375	1/15	6.3
D20L	25	500	1/20	4.8
D12E	25	300	1/12	7.7

The code L indicates powders obtained by evaporation and freeze-drying, whereas the code E denotes the formulation obtained by evaporation until dryness.

The solutions were then mixed under magnetic stirring to produce a transparent yellow mixture. The solvent was evaporated until it reached 15-20 ml using a rotary evaporator under reduced pressure at 95 °C. Finally, the resulting solutions were freeze-dried at −54.5°C under vacuum (0.909 mbar) for approximately 8 h, without the addition of cryoprotectants, using a Lio 5P Cinquepascale (Trezzano sul Naviglio, Italy). The freeze-drying process was carried out for 8 h. The formulation having a weight ratio quercetin/PVP10 of 1:12 (D12L) was selected as the leader one.

Moreover, a solid dispersion with the same quercetin/PVP10 weight ratio was also prepared evaporating by rotary evaporator, under reduced pressure at 95 °C, until dryness. The crumbly powder obtained was denoted as D12E.

2.3 Solubility studies

Excess amounts of pure quercetin or quercetin solid dispersions were dispersed into 2 ml of deionized water and the samples were kept shaking in a water bath at 20 °C. Powder of solid dispersion was added to water solution until clouding solution was observed, in order to verify the maximum solubility. The suspensions were filtered through a 0.22 µm syringe filter and an aliquot of 600 µl was mixed with the same volume of 20 mM water solution of NaOH.

Due to the chemical changes of quercetin in basic medium over time (Yang et al., 2010), quantification of the drug was performed after 40 min to allow stabilization of solution. According to Yang et al. (2010), the absorption bands of the reaction solution of quercetin and sodium hydroxide changed during the reaction due to the formation of intermediate and final products. After 40 min only the absorption band of the final product at 350 nm appeared.

The concentration of quercetin was determined by measuring the absorbance using UV–VIS spectrophotometer (Thermo Spectronic, Helios Gamma, England) at 350 nm. The calibration curve was linear in the range of 1–20.0 mg/L ($R^2 = 0.9999$).

2.4 *In vitro* characterization of solid dispersions D12L and D12E

2.4.1 Drug Content

191 The amount of quercetin entrapped within the solid dispersions was determined spectrophotometrically
192 by the same way as reported above. Briefly, 10 mg of each formulation were weighed accurately and
193 dissolved in 100 ml of 20 mM solution of NaOH. Then, the absorbance was read after 40 min and the
194 quercetin content was determined. The drug loading efficiency was then calculated as:

$$\text{Drug loading efficiency (\%)} = \frac{\text{Drug content (\% w/w)}}{\text{Theoretical drug content (\% w/w)}}$$

195
196
197
198
199 ***2.4.2 Particle size***
200 The particle size of D12L and D12E was determined using Coulter Laser Diffraction (Coulter LS 100
201 Q Laser Sizer, Beckman Coulter, Miami, FLA, USA). D12L or D12E was suspended in silicon oil
202 (Tegiloxan®). In both cases, sonication for 10 min was carried out. In addition, PVP10 (raw material)
203 dispersed in vaseline oil was analysed. Three dispersions were prepared for each formulation and the
204 values resulted from triplicate determinations of each dispersion (n=9). The average particle size was
205 expressed as the mean volume-surface diameter, d_{vs} (μm). The coefficient of uniformity (CU) was also
206 calculated by applying the following formula: CU = d10/d90 (Rassu et al., 2015). The values of d10
207 and d90 indicate, respectively, the particle diameter for which 10% and 90% of the particles have a
208 diameter less than the number indicated. A CU value approaching 1 indicates a dimensionally uniform
209 sample.
210
211 ***2.4.3 Density and flow properties***
212 The true density (ρ_t) of solid dispersions was calculated using a helium pycnometer AccuPyc II 1340
213 (Micromeritics®, GA, USA). An exactly weighed amount of each sample was filled in the sample cup.

214 ρ_t of the powder was determined for each batch as the ratio M/V_t, where M is the mass of the
215 dispersion powder and V_t is the average volume occupied with powder calculated with pycnometer
216 (Cerri et al., 2016).
217 The "bulk volume" V_{bulk} (i.e., volume of a given mass of powder filled into a graduated cylinder
218 without any compacting) and the "tapped volume" V_{tapped} of the powder (i.e., m/V50, where V50 is the
219 volume after 50 standardized taps) were also determined. The values of bulk density (ρ_{bulk}) and tapped
220 density (ρ_{tapped}) were calculated. The results were reported as the mean of three replicates for D12L and
221 D12E.
222 The Hausner's ratio (HR) and Carr's compressibility index (CI), used to predict powder flow
223 characteristics, were calculated according to following equations:

$$HR = \frac{\rho_{tapped}}{\rho_{bulk}}$$

$$CI\ (\%) = \frac{V_{bulk} - V_{tapped}}{V_{bulk}} \times 100$$

224 The results were compared with the scale of flowability given in the *Eur. Ph. 9th edition.*
225
226
227 ***2.4.4 X-ray powder diffraction***
228 X-ray powder diffraction (hereafter, XRPD) analyses of quercetin, PVP10, and solid formulations
229 D12L and D12E were performed using a Bruker D2-Phaser diffractometer (Karlsruhe, Germany).
230 Instrumental parameters were: CuKα radiation (λ = 0.15418 nm), 30kV, 10 mA, LynxEye PSD
231 detector set with an angular opening of 5°, 2θ range 5.8-70°, step size 0.020°, time per step 1 s, spinner
232 15 rpm. The alignment of the instrument was calibrated using the international standard NIST 1976b
233 (Gaithersburg, MD, USA). The analysis were performed at 26 ± 2 °C and 50 ± 2% of relative humidity,
234 conditions monitored with a Data Logger EBI20-TH1 (Ebro, Ingolstadt, Germany). A low-background
235 silicon crystal specimen holder, manufactured by Bruker (Karlsruhe, Germany), was used. The XRD

patterns were evaluated using the software Bruker EVA 14.2 (DIFFRAC^{plus} Package) coupled with the database PDF-2 (International Centre for Diffraction Data, Newtown Square, PA, USA).

2.4.5 Thermal analyses

Thermogravimetric and Differential Thermal Analyses (hereafter, TG and DTA) of quercetin, PVP10, and solid formulations D12L and D12E were performed using a Simultaneous Thermal Analyzer TA Instrument Q600 equipped with TA-Universal Analysis software (New Castle, DE, USA). About 7 mg of each sample was heated from room temperature to 500 °C under nitrogen flow (N_2 purity 99.999%) in an alumina crucible at the following operating conditions: 10 °C/min; gas flow 50 ml/min; an empty Al_2O_3 crucible was employed as reference. The software TA-Universal Analysis was used to evaluate the results.

2.4.6 Melting point determination

All melting points of pure substances (quercetin and PVP10) and solid formulations (D12L, D12E) were determined with a Kofler melting point apparatus. A physical mixture of drug and polymer (D12M) with weight ratio of 1:12 was prepared for comparison.

2.4.7 Fourier transform infrared spectroscopy (FT-IR)

Fourier transform infrared (FT-IR) spectroscopy was performed using (Avatar 320 FT-IR, Thermo Nicolet, Madison,WI, USA). FT-IR spectra for pure quercetin, polymer PVP10 and solid dispersions D12L and D12E were obtained using the KBr disk method. A physical mixture of drug and polymer (D12M) was again analysed for comparison.

2.5 Preparation and characterization of solutions

D12L and D12E solutions were prepared by solubilizing 200 mg of each solid formulation (containing about 16 mg of quercetin) in 1 ml of deionized water. D12L was also dissolved in saline solution at the same concentration in order to obtain the solution at the highest concentration employed for *in vivo* experiments. The final solutions were characterized in terms of pH at 20°C, osmolality and viscosity. The latter was determined at 20 °C by using Oswald U Tube viscometer. Osmolality was measured using an Osmomat 030 (Gonotec GmbH, Berlin, Germany). In addition, the injectability of water solutions of D12E and D12L and saline solution of D12L was evaluated by using a device made from a syringe and a pan resting on the piston of the syringe (Schuetz et al., 2008) with some modifications (Porcu et al., 2017).

2.5.1 Physical stability studies of water solutions

The solutions obtained by dissolving solid dispersions were characterized in terms of particle diameter using a Coulter nanosizer N5 (Beckman-Coulter Inc. Miami, FL, USA). With the aim of preparing aqueous solutions containing quercetin suitable for the injection, the particle size of D12E and D12L in water solution was used as the indicator to evaluate the physical stability of the formulations over time, at room temperature, up to 4 weeks.

2.5.2 Chemical stability studies of water solutions

Chemical stability studies were carried out on the injection formulations D12L and D12E in water at room temperature for a period of 28 days. In order to calculate the drug content, the samples were analysed spectrophotometrically, as reported above, at specific time intervals. The residual portion (%) of quercetin for each solution was calculated.

2.5.3 Sterilization

On the basis of the results obtained, D12L dissolved in saline was selected for further *in vivo* investigation. It was sterilized by autoclaving at 121 °C for 30 min. After that, the resulting solution was characterized in order to verify the influence of sterilization process on formulation properties. Parameters such as quercetin content, viscosity and injectability were determined in the same way as mentioned above.

2.6 *In vivo* studies

2.6.1 Animals and treatments

The experiments were carried out on male both conventional (normotensive) and spontaneously hypertensive rats. The animals were housed in the animal house of the Faculty of Pharmacy, Charles University, Czech Republic at a constant temperature 23-25°C, under a 12-h dark/light cycle. They were provided with a standard pellet diet and tap water ad libitum. The study (reg. No. MSMT-7041/2014-10) was approved by the Experimental Animal Welfare Committee of Charles University, Faculty of Pharmacy in Hradec Králové and conformed to The Guide for the Care and Use of Laboratory Animals, published by the US National Institutes of Health (NIH Publication No. 85-23, revised 1996).

2.6.2 Pharmacodynamic study

Six Wistar rats (Velaz, Czech Republic, average weight 415 ± 31 g, blood pressure values under anesthesia: 140 ± 25 / 75 ± 33 mmHg) were anesthetized i.p. by urethane (1.2 g kg^{-1}) and the arterial blood pressure and heart rate were recorded via a pressure transducer MLT0380/D linked to the right common carotid artery using PowerLab equipped with the software LabChart 7 (AdInstruments,

307 Australia). The *vena saphena sinistra* was cannulated and after an acclimatization period of 15 minutes,
308 D12L or pure polymer PVP10, both dissolved in saline, were administered as consequent bolus doses
309 (100 µl). In the case of D12L administration, the doses of pure quercetin were ranging from 0.05 mg
310 kg^{-1} to 5 mg kg^{-1} (corresponding to 0.65 to 65 mg kg^{-1} of D12L). The corresponding amount of PVP10
311 polymer was calculated for each dose and administered in the same volume as control. The experiment
312 was terminated by intravenous administration of 1 ml of 1 M KCl. The body temperature was
313 maintained during the whole experiment at 36.5 ± 0.5 °C.
314 Another fourteen, non-anesthetized, spontaneously hypertensive rats (Academy of Science, Czech
315 Republic, average weight 342 ± 15 g and initial systolic blood pressure value 177 ± 7 mmHg) were
316 treated intravenously with saline solution of D12L, via the tail vein (*vena caudalis*). The dose of
317 quercetin was 5 mg kg^{-1}. Equivalent amount of pure polymer PVP10 was also dissolved in saline and
318 served as the control. During the next 72 hours, the systolic blood pressure was non-invasively
319 monitored using the tail-cuff method (PowerLab coupled to a NIBP System, with a pulse transducer
320 and a tail occlusion cuff for rats, AdInstruments).
321
322 ***2.6.2 Pharmacokinetic study***
323 In additional three rats (average weight 359 ± 5 g) the plasma level of quercetin and its metabolites
324 were measured. Male Wistar rats under urethane anesthesia (the same dose as above) received *via vena*
325 *saphena sinistra* a dose of 5 mg/kg of D12L dissolved in saline. The blood samples in approximate
326 volumes of 350 µl were collected in subsequent time periods: 0; 1; 5; 10; 15; 30; 45; 60; 90; 120; 180
327 and 240 min. The blood samples were immediately centrifuged (2,500 g, 10 min, MPW-52, MPW
328 Med. Instruments, Poland) and the plasma samples were frozen at -80 °C for subsequent analysis.
329 The determination of quercetin and its metabolites including quercetin-3-O-glucuronide, tamarixetin
330 and isorhamnetin in these rat plasma was carried out using Acquity Ultra Performance LC ™ (UPLC)

system (Waters, Milford, MA, USA) coupled with Micromass Quattro micro ™ API benchtop triple quadrupole mass spectrometer (Waters, Milford, MA, USA). Analytical column BEH Shield RP C18 (2.1 × 100 mm, 1.7 µm) kept at 40 °C was employed for the separation of all analytes from matrix components. Compounds were separated using gradient elution with methanol and 0.1% formic acid at flow rate 0.35 mL min^{-1}. 5 µl of the extract were injected into the UHPLC-MS/MS system using the partial loop with needle overfill mode. All injected solutions were stored in the autosampler at 4 °C. The mass spectrometer parameters for electrospray ionization in positive mode were set up as follows: capillary voltage: 3.2 kV, RF lens voltage 0.5 V, extractor voltage 3.0 V, ion source temperature 130 °C, desolvation temperature 450 °C. The nitrogen cone gas flow was at 100 L h^{-1}; nitrogen desolvation gas flow at 800 L h^{-1}. Argon was used as a collision gas. Selected reaction monitoring (SRM) was used for quantification using precursor $[M+H]^+$ and a corresponding product ion in specific transitions: 303.0 > 153.0 for QCE (cone voltage 40.0 V and collision energy 30.0 eV), 479.2 > 303.1 for Q-3-Gl (cone voltage 25.0 V and collision energy 15.0 eV), and 317.2 > 302.0 for both TMX and IRN (cone voltage 40.0 V and collision energy 25.0 eV). The data were acquired using MassLynx 4.1 software (Waters) and processed by QuanLynx (Waters). The pretreatment of plasma samples consisted in simple protein precipitation, where acetonitrile acidified by 0.1% formic acid was added as precipitating agent rat plasma in 2:1 (v/v) ratio. Then, the sample was incubated for 10 min and consequently centrifuged for other 10 min. The supernatant was filtrated through 0.22 µm PTFE syringe filter and injected into the UHPLC system. The plasma samples containing quercetin and its metabolites were quantified using matrix calibration curve where the plasma samples were spiked by known amount of mentioned analytes.

2.7 Statistical analysis

Statistical analysis was performed with GraphPad Prism 6.02. Comparison between two groups was performed by Mann-Whitney test, while among more groups was carried out using Kruskal-Wallis test following Dunn's Multiple Comparison Test. The differences in blood pressure in relation to time (tail-cuff method) were compared by the use of two-way ANOVA. The significance level was set at $p < 0.05$, if not state otherwise. Data are shown in both *in vitro* and *in vivo* experiments as mean ± SD. For *in vitro* studies, at least triplicates were performed. The number of animals, used for *in vivo* studies, is mentioned in the corresponding parts of the article.

3. RESULTS AND DISCUSSION

3.1 Solubility studies

The co-solvent evaporation technique was employed for the preparation of solid dispersions in order to improve quercetin solubility in water. The solubility data indicated that the solubility of quercetin depends on the drug/polymer ratio employed. As shown in Fig. 1, formulations prepared with drug/polymer weight ratio of 1:12 were associated with maximal improvement in quercetin water solubility, regardless of preparation method used. In fact, D12L and D12E were prepared by co-solvent evaporation method, but in the case of D12L this step was followed by freeze-drying process. Nevertheless, in both formulations the solubility of quercetin increased almost 20,000 fold. Indeed, in the case of D12L/D12E solid dispersions, the water solubility quercetin increased to 41.6 mg/ml, which was much higher than that of anhydrous solubility (0.00215 g/L at 25 °C), as reported by Srinivas et al. (2010).

The use of larger amount of PVP in D15L and D20L compared to 1:12 weight ratio, resulted in solutions with very high viscosity; these systems were, therefore, not suitable for the preparation of parenteral injections. For this reason, D12L and D12E were chosen as leader formulations for the further studies.

3.2 In vitro characterization of solid dispersions D12L and D12E

3.2.1 Drug content, drug loading efficiency and particle size

Drug content studies showed that the real content of quercetin loaded in D12L and D12E was slightly lower than the theoretical values (Supplementary Table S2), but the mean values of drug loading efficiencies were above 90 % for both formulations.

The sizes of solid dispersion particles were compared. D12L particles tended to have a larger volume-surface diameter (d_{vs}) than D12E particles (Supplementary Fig. S1) but no significant differences were observed ($p > 0.05$). In both cases, the formation of solid dispersion led to a decrease in particle size of the polymer. Indeed preparation of solid dispersions leads to reduction of particle size to molecular level. This aspect has an important impact on solubility. When the soluble carrier dissolves, the insoluble drug is exposed to the dissolution medium in the form of very fine particles with increased contact area, allowing its quick dissolution and absorption (Sharma and Jain, 2010). Solid dispersions and PVP particles showed a wide size distribution, as indicated by low CU values ($CU < 0.15$) reported in Supplementary Table S1, that decreased in the order D12E > D12L > PVP. Therefore, D12E was the most uniform preparation in size, with a CU value nearer to 1 in comparison to other samples. The particle distribution for all three samples is shown in Supplementary Fig. S1.

3.2.2 Density and flow properties

The values of density and flow properties are reported in Supplementary Table S2. The true density of D12L and D12E solid dispersions were similar (1.301 ± 0.008 *vs* 1.230 ± 0.002 g/cm^3) ($p > 0.05$). The freeze-drying process increased markedly the bulk volume of D12L compared to D12E ($p < 0.05$). The flowability of the solid dispersions was determined using Hausner's ratio and compressibility index. A Carr's CI of < 10 or HR of < 1.11 are considered 'excellent' flow whereas CI > 38 or HR > 1.60 are considered 'very very poor' flow according to *Eur. Ph.* D12L showed little inclination to flow (Supplementary Table S2). The HR and the CI were 1.626 ± 0.035 and 38.99 ± 1.554, respectively, hence D12L exhibited "extremely poor" flowability. On the contrary, D12E showed good flowability as confirmed by good values of HR (1.092 ± 0.037) and CI (8.59 ± 2.89). Therefore, preparation technique affected the powder properties. In spite of high volume occupied by the powder, D12L shows good properties for a possible compression. This aspect confirms that the formulation can be proposed not only as solution, but also as powder to improve stability. On the contrary, D12E exhibited a lower bulk volume, favoring a practical package.

3.2.3 X-ray powder diffraction

The diffractograms of the samples are illustrated in Fig. 2. The XRPD pattern of quercetin showed a set of sharp peaks corresponding to three crystalline forms of quercetin, namely dihydrate (triclinic, space group P-1; PDF number 43-1695), anhydrous (monoclinic, space group $P2_1/a$; Filip et al., 2013), and a second anhydrous polymorph with structure not yet identified (peaks at 2θ values of 7.6°, 9.4°, 12.9°, 14.0°, 22.1°, and 28.3°; Trendafilova et al., 2017). The coexistence of more forms of quercetin in raw materials supplied by pharmaceutical companies was already reported (Borghetti et al., 2012; Trendafilova et al., 2017).

PVP is an amorphous material, and its diffraction pattern presents two halos whose angular positions change with the adsorption of water (Teng et al., 2010). PVP10 showed two maximum at, respectively, 11.7° and 20.4° 2θ (Fig. 2), values in good agreement with those reported for a PVP of low molecular weight (PVP K-12) measured at ambient temperature and 53% of relative humidity (Teng et al., 2010). Basically, the XRPD patterns D12L and D12E resulted identical to PVP10, thus revealing the amorphous structure of the two formulations. Therefore, preparation technique did not influence XRPD patterns of solid dispersions.

3.2.4 Thermal analyses

The TG and DTA curves of the samples are reported in Fig. 3. The DTA path of quercetin exhibited a weak endothermic peak at 46.7 °C, linked to the evolution of adsorbed water (weight loss of 1.3% along the TG curve), followed by a more evident endothermic event at 108.9 °C, determined by the loss (3.1%) of H_2O molecules from the crystal lattice of the hydrate form of quercetin. The drug exhibited a third endothermic reaction, marked by the sharp peak at 318.0 °C, related to the melting of the flavonoid, whereas the exothermic event at 343.8 °C, accompanied by a weight loss of about 23.7%, is related to quercetin degradation process (Borghetti et al., 2012). Quercetin showed a residual mass of 57.1% at 500 °C. PVP10 displayed two main endothermic reactions: at 66.3 °C, associated to the loss of adsorbed water (10.8%), and at 430.9 °C, caused by the decomposition of the polymer whose residual mass at 500 °C was 2.1%. The TG-DTA curves of the formulations D12L and D12E turned out almost identical to each other, and very similar to those of PVP10. The first endothermic reaction occurred at 64.7 °C for D12L and at 66.9 °C for D12E, the second endothermic event between 434.1 °C (D12L) and 434.5 °C (D12E). At 500 °C, D12L evidenced a residual mass of 8.0%, a bit higher than D12E (5.6%), a difference consistent with the drug content measured in the two formulations, slightly superior in D12L (see Supplementary Table S1).

449 ***3.2.5 Melting point determination***

450 Both solid dispersions showed different melting points compared to single components (PVP10:
451 165°C-170°C and quercetin: 305°C-307°C), confirming the formation of interactions between them.
452 The physical mixture D12M containing quercetin and PVP10 displayed higher melting point (210°C-
453 220°C) than D12L (180°C-185°C) and D12E (175°C-180°C).

454

455 ***3.2.6 FT-IR***

456 The FT-IR spectra of quercetin, PVP, the solid dispersions D12L and D12E and physical mixture
457 D12M were recorded in order to investigate the possible chemical interactions between the drug and
458 the polymer in the solid dispersion formulation (Fig. 4). The spectra of quercetin exhibited a strong and
459 broad stretching absorbance peak at 3405 cm^{-1} due to hydroxyl groups, which might form inter-
460 molecular hydrogen bonds with the phenolic –OH groups and aromatic ketone moiety. In addition, the
461 stretching vibration peak of C=O aryl ketonic group was found at 1664 cm^{-1} (Pralhad and
462 Rajendrakumar, 2004). Other characteristic peaks in the quercetin molecule due to C=C aromatic ring
463 stretching were detectable at 1610, 1560, and 1510 cm^{-1} as reported previously in literature (Catauro
464 2015, Borghetti et al., 2009). Band at 1319 cm^{-1} was attributable to C–H bending in aromatic
465 hydrocarbon, as well as peaks at 940, 825, 680 and 600 cm^{-1}.
466 PVP exhibits a characteristic peak at the frequency 1655 cm^{-1}, relative to the stretching of amide
467 carbonyl group of the PVP units. Other peaks at 2958 cm^{-1} as a result of C_{sp}^{3}-H stretching and at 3448
468 cm^{-1}, owing to N-H stretching were exhibited in FTIR spectra of polymer (De Mello Costa et al., 2010;
469 Zhu et al., 2007). The peak at 1290 cm^{-1} typical for C–N bond in PVP was also presented. The peak at
470 1655 cm^{-1} was characteristic for carbonyl group of PVP (Bryaskova et al., 2011).
471 FT-IR patterns of D12L and D12E were compared with pure quercetin and PVP spectra. Although
472 D12L showed a peak of lower amplitude at 3448 cm^{-1}, in both cases, solid dispersions spectra were

more similar to the polymer spectrum (peaks at 3448, 2955 and 1650-1670 cm^{-1}) (Fig. 4). Almost all peaks of quercetin shifted, decreased in intensity or totally disappeared, which suggests that hydrogen bonding occurs between quercetin and PVP (Li X.Y. et al. 2013; Yan et al., 2014).

The FTIR spectra of physical mixture D12M seemed to be only a summation of quercetin and PVP spectra. This aspect suggested that there was no interaction between drug and polymer in the physical mixture.

3.3 Characterization of solutions

D12L and D12E solubilized in water and D12L in saline solution were analyzed in terms of pH, osmolality and viscosity. As reported in Supplementary Table S3, the values of both formulations were very similar. The pH was acidic for both solutions (about 4) and therefore they are suitable for intravenous administration, which requires the pH in range of 4 to 8 (Tihanyi and Vastag, 2011). As confirmed by countless animal studies, a solution with a pH of 3-11 did not induce phlebitic changes, when drugs were administered over a few minutes (Roethlisberger et al., 2017). The viscosity of solutions was determined: solutions containing 200 mg/ml of solid dispersion showed values up to 3 centipoises (Table S3 for Supplementary data). Nevertheless, diluted solutions with lower concentration of quercetin, used for *in vivo* experiments, exhibited low viscosities, comparable to the value of saline solution (1 cP) (Berteau et al., 2015).

The osmolality of solutions was measured (Supplementary Table S3), confirming the suitability of D12L in saline solution for injection (415.2 ± 3.1 mOsmol/kg). Injectable of < 600 mOsm/kg is considered to have a low-to-moderate risk of phlebitis; in particular, solutions with an osmolality less than 450 mOsm/kg are generally well tolerated by intravenous administration.

Nevertheless, very hypotonic solutions cause swelling of red blood cells and hemolysis, associated with pain and physiologic disturbances (Wang, 2015). Therefore, solid dispersions dissolved in water should not be administered (Supplementary Table S3).

The injectability of all solutions tested in *in vivo* experiments (200 mg/ml, 100 mg/ml, 40 mg/ml, 20 mg/ml, 8 mg/ml, 4 mg/ml, 2 mg/ml) was evaluated by using the method reported by Schuetz et al. (2008) with some modifications. Injectability concept includes pressure or force required for injection, evenness of flow, and freedom from clogging (Cilurzo et al., 2011).

As expected, the injection speed rate was dependent on the concentration of samples; however, no solutions met any resistance. Obviously, injectability was related to product viscosity; indeed higher values of force required to push the solution through the syringe with more concentrated solutions compared to saline were obtained, by the virtue of PVP that increase the viscosity of solution (data not shown).

3.3.1 Physical stability studies of water solutions

Physical stability studies showed that aqueous solutions obtained from solid dispersions were quite stable over time. In fact, particle size of D12E increased from 20 nm to 100 nm after 28 days of storage at room temperature, as reported in Supplementary Fig. S2. Noteworthy, D12L was more stable than D12Es, showing a little increase in mean diameter until the 3th week, with no further changes during the last week of storage. Nevertheless, both solutions showed similar properties. Taking into account the data obtained, aggregation or precipitation of quercetin did not occur and thus a good stability of the drug in solution was supposed.

3.3.2 Chemical stability studies of water solutions

The drug contents of both solutions were determined spectrophotometrically over time in order to assess their chemical stability. During the 1st and 2nd weeks, the formulations were quite stable but after 4 weeks, a rate of quercetin degradation corresponding to 30% was observed (data not shown). This behavior can negatively influence the therapeutic effect of the formulations. The product may be susceptible to physical and chemical degradation when stored as a ready-to-use solution. Therefore, considering the results obtained, the reconstitution of the powder prior to administration is highly recommended.

3.4 Sterilization

Sterilization process, required for injectable administration, did not modify the properties of D12L formulation dissolved in saline in terms of quercetin content, viscosity and injectability, confirming the feasibility of the process on the reconstituted powder (data not showed).

3.5 In vivo studies

By comparing the results from the *in vitro* characterization of the two solid dispersions, there are no or minor differences between D12E and D12L. Therefore, D12L was selected for *in vivo* studies because freeze-dried powders are more suitable and accepted for parenteral formulations.

Intravenous administration of D12L solid dispersion dissolved in saline led to decreases in both systolic and diastolic blood pressures in all anesthetized animals, however the dose of quercetin necessary for a blood pressure response was variable and ranged between 0.1 and 2.5 mg kg^{-1} (Fig. Supplementary Data S3A). Pure polymer had apparently very little influence on the blood pressure in this acute experiments. Comparison of maximal pressure drop between D12L and the control is shown in Fig. 5A.

541 Concerning the kinetics of blood pressure changes, the pressure started to decrease 2-3 minutes after
542 the i.v. application of D12L and importantly the effect was gradual and persistent after one dose.
543 Diastolic pressure tended to decrease more than systolic (Fig. 5B) in line with the assumption that
544 quercetin acts in this acute experiments at the level of the vascular system. However, due to variable
545 responses among animals, this change was not significant. The heart rate was not significantly
546 influenced after administration of neither pure polymer solution nor quercetin dispersions (Fig.
547 Supplementary Data S3B).
548 Pure quercetin is known to have vasodilatory effects on vascular smooth muscle cells *ex vivo* (Duarte et
549 al., 1993); however its oral administration results in negligible concentrations of pure (non-
550 metabolized) quercetin in plasma and its major conjugated metabolites had no direct vasodilatory
551 effects neither *ex vivo* (quercetin-3-O-glucuronide, quercetin-3´-sulfate) (Lodi et al., 2009; Najmanová
552 et al., 2016) nor *in vivo* (quercetin-3´-sulfate) (Galindo et al., 2012). In our experiments, a solid
553 dispersion system carrying pure quercetin was used in order to demonstrate the *in vivo* direct
554 vasodilatory activity of quercetin, administered in a biologically compatible solvent. Indeed, the arterial
555 blood pressure decrease was observed few minutes after D12L intravenous administration. As
556 mentioned, there was a marked difference between tested animals, for most of them the dose of 1 or 2.5
557 mg kg^{-1} of quercetin was needed to evoke a drop in arterial blood pressure. Because of these
558 differences, we did not continue in dose-response studies, but the single dose of 5 mg kg^{-1} of quercetin
559 was selected for further confirmation of direct quercetin vasodilatory activity, in non-anesthetized,
560 spontaneously hypertensive animals. Also in this case, the intravenous administration of D12L caused a
561 decrease in systolic blood pressure (Fig. 6). The decrease started approximately 1 hour after
562 administration and continued during the next 4 hours, reached an approximately 30% reduction of the
563 initial blood pressure. After that, the systolic blood pressure slowly returned to the initial values.
564 Interestingly, some decrease in blood pressure (10-20%) was observed also in the case of pure polymer,

but the effect of quercetin, given as D12L, was apparently stronger and reached significant difference *vs.* PVP10 at 3-5 hours after the administration. The explanation why the pure polymer caused also a decrease in arterial blood pressure is not known. Few papers described the PVP effect on the vascular system. Similarly to our study, PVP caused a profound decrease of blood pressure in dogs. Likely vasodilation and increased capillary permeability were responsible for the effect (Marshall and Hanna, 1957). In another article, an increase in eNOS levels in aortic endothelial cells was reported after PVP administration to female rats, and the Rho-ROCK pathway was hypothesized to contribute to this vascular response. However, mostly non-consistent and non-significant tendencies in the contractile response of arteries were found *ex vivo*, and the results varied between pregnant and non-pregnant animals (Vidanapathirana, 2014). On the other hand, also results showing decreased ACh vasodilator response due to PVP are available (Mohamed, 2017).

As the last part, the analysis of pharmacokinetics of i.v. given D12L formulation was carried out. In addition to quercetin, also its metabolites appeared in plasma (Fig.7). Rapid decrease in plasma concentrations of quercetin with appearance of its known metabolites suggest that quercetin given in this formulation is rapidly dissolved in plasma similarly as it would be expected after administration of homogenous quercetin solution (e.g. by use of organic solvents). Concerning metabolites, isorhamnetin reached 10 times lower plasma concentrations than quercetin while its maximal concentration was more than 3 times higher than that of quercetin-3-O-glucuronide. Only very low concentrations of tamarixetin were observed.

There are no human studies, in which quercetin was given i.v. in a biologically compatible solvent. There is one clinical study in which large doses of quercetin dissolved in DMSO were given (Ferry et al., 1996). However, such administration cannot be used for tracking the effect of quercetin since DMSO can have negative effects.

588 Summarizing both pharmacodynamics experiments from this study, the arterial blood pressure started
589 to decrease one hour after D12L i.v. administration, while similar blood-pressure lowering effects in
590 anesthetized rats were observed within few minutes. This discrepancy can be related to both 1) the
591 difference between the two types of experiments, with anesthetized and awake animals, and 2) the
592 different mechanisms of action. For awake animals, the intravenous administration always represents a
593 stress, even if it is performed in a gently way. Additionally, the blood pressure was measured by the
594 occlusion cuff on the tail, which was also the place of application. Moreover, the repeated
595 measurements at the beginning of the experiment in quick succession, could be another stress factor
596 (even if the rats were previously trained for 2 weeks to adapt to this procedure). Despite these
597 disadvantages, experiments on awake animals allow long-term monitoring of the studied effects that
598 would not be realizable in animals under general anesthesia, and further confirmed the effect of
599 quercetin. The acute and later effects of flavonoids on arterial blood pressure might be different.
600 Acutely, flavonoids relax directly arteries while in a long-term base, they can have an effect on
601 pathophysiology of hypertension. In terms of acute effects, there is no difference between quercetin and
602 both its methylated metabolites isorhamnetin and tamarixetin while as mentioned above, quercetin-3-
603 O-glucuronide is inactive (Najmanová et al., 2016). Regarding the later hypotensive effect, there are
604 more suggested mechanisms. Quercetin is able to induce concentration-dependent phosphorylation of
605 endothelial NO-synthase with subsequent improvement of vasodilation, both quercetin and
606 isorhamnetin can decrease the expression of a NADPH-oxidase subunit, while isorhamnetin and
607 quercetin-3-O-glucuronide, but not quercetin itself, are also blocking this enzyme (Chirumbolo, 2012;
608 Mladěnka et al., 2010; Romero et al., 2009; Steffen et al., 2008). Hence the effect observed in this
609 study in rats might be mediated not only by quercetin but also by its metabolites. In order to analyse the
610 contribution of the metabolite(s), similar water-soluble preparation of isorhamnetin, in particular, will
611 be needed, since isorhamnetin was apparently the major metabolite of quercetin given as D12L.

4. CONCLUSION

In this manuscript the authors described the preparation and characterization of solid dispersion enabling solubilization of quercetin in aqueous media for investigation of its direct *in vivo* cardiovascular effects. Low water solubility of quercetin represents a limit for testing and subsequent use of the drug. The *in vitro* characterization of the two solid dispersions prepared by using different techniques showed no important differences in both powder and solution forms. The solid dispersion prepared can be easily solubilized in aqueous media. However, considering the obtained results, the reconstitution of the formulation from freeze-dried powder before administration is highly recommended.

This study gives also a direct proof of in vivo effects of i.v. given quercetin. Quercetin, administered in this i.v. way, reduced the arterial blood pressure in both awake and anesthetized rats. Nevertheless, rapid decrease of quercetin plasma concentration was observed after *in vivo* administration of solid dispersion. Hence metabolites, in particularly isorhamnetin and possibly quercetin-3-O-glucoronide, could contribute to the vasodilatory effect of quercetin.

Acknowledgements

The authors gratefully acknowledge the financial support of the GACR 17-05409S/P301 and the project STARSS reg. no.: CZ.02.1.01/0.0/0.0/15_003/0000465 funded by EFRR.

Conflicts of interest

The authors declare no conflicts of interest.

636 **REFERENCES**

637 Alves, L.D.S., Soares, M.F.D.L.R., de Albuquerque, C.T., da Silva, É.R., Vieira, A.C.C., Fontes,
638 D.A.F., Figueirêdo, C.B.M., Sobrinho J.L.S., Neto, P.J.R., 2014. Solid dispersion of efavirenz in PVP
639 K-30 by conventional solvent and kneading methods. Carbohydr. Polym. 104, 166-174.

640 Borghetti, G.S., Carini, J.P., Honorato, S.B., Ayala, A.P., Moreira, J.C.F., Bassani, V.L., 2012.
641 Physicochemical properties and thermal stability of quercetin hydrates in the solid state. Thermochim.
642 Acta. 539, 109-114.

643 Borghetti, G.S., Lula, I.S., Sinisterra, R.D., Bassani, V.L., 2009). Quercetin/β-Cyclodextrin solid
644 complexes prepared in aqueous solution followed by spray-drying or by physical mixture. AAPS
645 PharmSciTech. 10, 235-242.

646 Bose, S., Du, Y., Takhistov, P., Michniak-Kohn, B., 2013. Formulation optimization and topical
647 delivery of quercetin from solid lipid based nanosystems. Int. J. Pharm. 441, 56-66.

648 Bryaskova, R., Pencheva, D., Nikolov, S., Kantardjiev, T., 2011. Synthesis and comparative study on
649 the antimicrobial activity of hybrid materials based on silver nanoparticles (AgNps) stabilized by
650 polyvinylpyrrolidone (PVP). J. Chem. Biol. 4, 185-191.

651 Caddeo, C., Nacher, A., Vassallo, A., Armentano, M.F., Pons, R., Fernàndez-Busquets, X., Carbone,
652 C., Valentia, D., Fadda, A.M., Manconi, M., 2016. Effect of quercetin and resveratrol co-incorporated
653 in liposomes against inflammatory/oxidative response associated with skin cancer. Int. J. Pharm. 513,
654 153-163.

655 Catauro, M., Papale, F., Bollino, F., Piccolella, S., Marciano, S., Nocera, P., Pacifico, S., 2015.
656 Silica/quercetin sol–gel hybrids as antioxidant dental implant materials. Sci. Technol. Adv. Mater. 16,
657 035001.

Cerri, G., Farina, M., Brundu, A., Daković, A., Giunchedi, P., Gavini, E., Rassu, G., 2016. Natural zeolites for pharmaceutical formulations: Preparation and evaluation of a clinoptilolite-based material. Microporous Mesoporous Mater. 223, 58-67.

Cilurzo, F., Selmin, F., Minghetti, P., Adami, M., Bertoni, E., Lauria, S., Montanari, L., 2011. Injectability evaluation: an open issue. AAPS Pharm. Sci. Tech. 12, 604-609.

Chirumbolo, S., 2012. Role of quercetin in vascular physiology. Can. J. Physiol. Pharmacol. 90, 1652-1657.

Date, A.A., Nagarsenker, M.S., 2008. Parenteral microemulsions: an overview. Int. J. Pharm. 355, 19-30.

de Mello Costa, A.R., Marquiafavel, F.S., de Oliveira Lima Leite Vaz, M.M., Rocha, B.A., Pires Bueno, P.C., Amaral, P.L.M., da Silva Barud, H., Berreta-Silva, A. A., 2010. Quercetin-PVP K25 solid dispersions: preparation, thermal characterization and antioxidant activity. J. Therm. Anal. Calorim. 104, 273-278.

Del Rio, D., Rodriguez-Mateos, A., Spencer, J.P., Tognolini, M., Borges, G., Crozier, A., 2013. Dietary (poly) phenolics in human health: structures, bioavailability, and evidence of protective effects against chronic diseases. Antioxid. Redox Signal. 18, 1818-1892.

Duarte, J., Vizcaíno, F.P., Utrilla, P., Jiménez, J., Tamargo, J., Zarzuelo, A., 1993. Vasodilatory effects of flavonoids in rat aortic smooth muscle. Structure-activity relationships. Gen. Pharmacol. 24, 857-862.

Eur Ph. Pharmaceutical Technical Procedures (Chapter 2.9) European Pharmacopoeia 8.0, 01/2014, Convention, Strasbourg, France (2014), pp. 285-370.

679 Ferry, D.R., Smith, A., Malkhandi, J., Fyfe, D.W., Anderson, D., Baker, J., Kerr, D.J., 1996. Phase I
680 clinical trial of the flavonoid quercetin: pharmacokinetics and evidence for in vivo tyrosine kinase
681 inhibition. Clin. Cancer Res. 2, 659-668.

682 Filip, X., Grosu, I.G., Miclăuş, M., Filip, C., 2013. NMR crystallography methods to probe complex
683 hydrogen bonding networks: application to structure elucidation of anhydrous quercetin. Cryst. Eng.
684 Comm. 15, 4131-4142.

685 Folttmann, H., Quadir, A., 2008. Polyvinylpyrrolidone (PVP)-one of the most widely used excipients
686 in pharmaceuticals: an overview. Drug Deliv. Technol. 8, 22–27.

687 Galindo, P., Rodriguez-Gómez, I., González-Manzano, S., Dueñas, M., Jiménez, R., Menéndez, C.,
688 Vargas, F., Tamargo, J., Santos-Buelga, C., Pérez-Vizcaíno, F., Duarte, J., 2012. Glucuronidated
689 quercetin lowers blood pressure in spontaneously hypertensive rats via deconjugation. PloS one. 7,
690 e32673.

691 Gao, X., Wang, B., Wei, X., Men, K., Zheng, F., Zhou, Y., Zheng, Y., Gou, M., Huang, M., Guo, G.,
692 Huang, N., Qian, Z., Wei, Y., 2012. Anticancer effect and mechanism of polymer micelle-encapsulated
693 quercetin on ovarian cancer. Nanoscale. 4, 7021-7030.

694 Gao, Y., Wang, Y., Ma, Y., Yu, A., Cai, F., Shao, W., Zhai, G., 2009. Formulation optimization and in
695 situ absorption in rat intestinal tract of quercetin-loaded microemulsion. Colloids Surf. B Biointerfaces.
696 71, 306-314.

697 Gilley, A.D., Arca, H.C., Nichols, B.L., Mosquera-Giraldo, L.I., Taylor, L.S., Edgar, K.J., Neilson,
698 A.P., 2017. Novel cellulose-based amorphous solid dispersions enhance quercetin solution
699 concentrations in vitro. Carbohydr. Polym. 157, 86-93.

700 Hädrich, G., Vaz, G.R., Maidana, M., Kratz, J.M., Loch-Neckel, G., Favarin, D.C., de Paula Rogerio,
701 A., Rodrigues, F.M., da Silva, F.M.R., Muccillo-Baisch, A.L., Dora, C.L., 2016. Anti-inflammatory
702 effect and toxicology analysis of oral delivery quercetin nanosized emulsion in rats. Pharm. Res. 33,
703 983-993.

704 Jahangiri, A., Barzegar-Jalali, M., Garjani, A., Javadzadeh, Y., Hamishehkar, H., Afroozian, A.,
705 Adibkia, K., 2015. Pharmacological and histological examination of atorvastatin-PVP K30 solid
706 dispersions. Powder Technol., 286, 538-545.

707 Jullian, C., Moyano, L., Yanez, C., Olea-Azar, C., 2007. Complexation of quercetin with three kinds of
708 cyclodextrins: an antioxidant study. Spectrochim. Acta A Mol. Biomol. Spectrosc. 67, 230-234.

709 Kadajji, V.G., Betageri, G.V., 2011. Water soluble polymers for pharmaceutical applications.
710 Polymers. 3, 1972-2009.

711 Kakran, M., Sahoo, N.G., Li, L., 2011. Dissolution enhancement of quercetin through nanofabrication,
712 complexation, and solid dispersion. Colloids Surf. B Biointerfaces. 88, 121-130.

713 Kumar, P., Sharma, G., Kumar, R., Singh, B., Malik, R., Katare, O.P., Raza, K., 2016. Promises of a
714 biocompatible nanocarrier in improved brain delivery of quercetin: Biochemical, pharmacokinetic and
715 biodistribution evidences. Int. J. Pharm. 515, 307-314.

716 Kumar, S., Pandey, A. K., 2013. Chemistry and biological activities of flavonoids: an overview. Sci.
717 World J. 2013, doi:10.1155/2013/162750.

718 Larson, A.J., Symons, J.D., Jalili, T., 2010. Quercetin: a treatment for hypertension?—a review of
719 efficacy and mechanisms. Pharmaceuticals, 3(1), 237-250.

720 Li, B., Konecke, S., Harich, K., Wegiel, L., Taylor, L.S., Edgar, K.J., 2013. Solid dispersion of
721 quercetin in cellulose derivative matrices influences both solubility and stability. Carbohydr. Polym.
722 92, 2033-2040.

723 Li, H., Zhao, X., Ma, Y., Zhai, G., Li, L., Lou, H., 2009. Enhancement of gastrointestinal absorption of
724 quercetin by solid lipid nanoparticles. J. Control. Release. 133, 238-244.

725 Li, X.Y., Li, Y.C., Yu, D.G., Liao, Y.Z., Wang, X., 2013. Fast disintegrating quercetin-loaded drug
726 delivery systems fabricated using coaxial electrospinning. Int. J. Mol. Sci. 14, 21647-21659.

727 Lodi, F., Jimenez, R., Moreno, L., Kroon, P.A., Needs, P.W., Hughes, D.A., Santos-Buelga, C.,
728 Gonzalez-Paramas, A., Cogolludo, A., Lopez-Sepulveda, R., Duarte, J., Perez-Vizcaino, F., 2009.
729 Glucuronidated and sulfated metabolites of the flavonoid quercetin prevent endothelial dysfunction but
730 lack direct vasorelaxant effects in rat aorta. Atherosclerosis. 204, 34-39.

731 Marshall, L.H., Hanna, C.H., 1957. Circulatory reaction of tolerant and nontolerant dogs to
732 polyvinylpyrrolidone and of rats to dextran. Am. J. Physiol. 189, 209-213.

733 Mladěnka, P., Zatloukalová, L., Filipský, T., Hrdina, R., 2010. Cardiovascular effects of flavonoids are
734 not caused only by direct antioxidant activity. Free Radic. Biol. Med. 49, 963-975.

735 Mohamed, T., Matou-Nasri, S., Farooq, A., Whitehead, D., Azzawi, M., 2017. Polyvinylpyrrolidone-
736 coated gold nanoparticles inhibit endothelial cell viability, proliferation, and erK1/2 phosphorylation
737 and reduce the magnitude of endothelial-independent dilator responses in isolated aortic vessels. Int. J.
738 Nanomed. 12, 8813- 8830.

739 Najmanová, I., Pourová, J., Vopršalová, M., Pilařová, V., Semecký, V., Nováková, L., Mladěnka, P.,
740 2016. Flavonoid metabolite 3- (3- hydroxyphenyl) propionic acid formed by human microflora
741 decreases arterial blood pressure in rats. Mol. Nutr. Food Res. 60, 981-991.

742 Otto, D.P., Otto, A., de Villiers, M.M., 2013. Experimental and mesoscale computational dynamics
743 studies of the relationship between solubility and release of quercetin from PEG solid dispersions. Int.
744 J. Pharm. 456, 282-292.

745 Park, S.H., Song, I.S., Choi, M.K., 2016. Preparation and Characterization of Quercetin-Loaded Solid
746 Dispersion by Solvent Evaporation and Freeze-Drying Method. Mass Spectrometry Letters. 7, 79-83.

747 Pralhad, T., Rajendrakumar, K., 2004. Study of freeze-dried quercetin–cyclodextrin binary systems by
748 DSC, FT-IR, X-ray diffraction and SEM analysis. J. Pharm. Biomed. Anal. 34, 333-339.

749 Porcu, E.P., Salis, A., Rassu, G., Maestri, M., Galafassi, J., Bruni, G., Giunchedi, P., Gavini, E., 2017.
750 Engineered polymeric microspheres obtained by multi-step method as potential systems for
751 transarterial embolization and intraoperative imaging of HCC: Preliminary evaluation. Eur. J. Pharm.
752 Biopharm. 117, 160-167.

753 Puerta, E., Suárez-Santiago, J.E., Santos-Magalhães, N.S., Ramirez, M.J., Irache, J. M., 2017. Effect of
754 the oral administration of nanoencapsulated quercetin on a mouse model of Alzheimer's disease. Int. J.
755 Pharm. 517, 50-57.

756 Rassu, G., Soddu, E., Cossu, M., Brundu, A., Cerri, G., Marchetti, N., Ferraro, L., Regan, R.F.,
757 Giunchedi, P., Gavini, E., Dalpiaz, A., 2015. Solid microparticles based on chitosan or methyl-β-
758 cyclodextrin: A first formulative approach to increase the nose-to-brain transport of deferoxamine
759 mesylate. J. Control. Release. 201, 68-77.

760 Roethlisberger, D., Mahler, H.C., Altenburger, U., Pappenberger, A., 2017. If euhydric and isotonic do
761 not work, what are acceptable pH and osmolality for parenteral drug dosage forms? J. Pharm. Sci. 106,
762 446-456.

763 Romero, M., Jiménez, R., Sánchez, M., López-Sepúlveda, R., Zarzuelo, M.J., O'Valle, F., Zarzuelo,
764 A., Pérez-Vizcaíno, F., Duarte, J., 2009. Quercetin inhibits vascular superoxide production induced by
765 endothelin-1: Role of NADPH oxidase, uncoupled eNOS and PKC. Atherosclerosis. 202, 58-67.

766 Sansone, F., Picerno, P., Mencherini, T., Villecco, F., D'ursi, A.M., Aquino, R.P., Lauro, M.R., 2011.
767 Flavonoid microparticles by spray-drying: Influence of enhancers of the dissolution rate on properties
768 and stability. J. Food Eng. 103, 188-196.

769 Sareen, S., Mathew, G., Joseph, L., 2012. Improvement in solubility of poor water-soluble drugs by
770 solid dispersion. Int. J. Pharm. Investig. 2, 12-17.

771 Schuetz, Y.B, Gurny, R., Jordan, O., 2008. A novel thermoresponsive hydrogel based on chitosan, Eur.
772 J. Pharm. Biopharm. 68, 19–25.

773 Sethia, S., Squillante, E., 2004. Solid dispersion of carbamazepine in PVP K30 by conventional solvent
774 evaporation and supercritical methods. Int. J. Pharm. 272, 1-10.

775 Sharma, A., Jain, C.P., 2010. Preparation and characterization of solid dispersions of carvedilol with
776 PVP K30. Res. Pharm. Sci. 5, 49-56.

777 Smith, A.J., Kavuru, P., Wojtas, L., Zaworotko, M.J., Shytle, R.D., 2011. Cocrystals of quercetin with
778 improved solubility and oral bioavailability. Mol. Pharm. 8, 1867-1876.

779 Soni, L.K., Solanki, S.S., Maheshwari, R.K., 2014. Solubilization of poorly water soluble drug using
780 mixed solvency approach for aqueous injection. Br. J. Pharm. Res. 4, 549-568.

781 Sri, K.V., Kondaiah, A., Ratna, J.V., Annapurna, A., 2007. Preparation and characterization of
782 quercetin and rutin cyclodextrin inclusion complexes. Drug Dev. Ind. Pharm. 33, 245-253.

783 Srinivas, K., King, J.W., Howard, L. R., Monrad, J. K., 2010. Solubility and solution thermodynamic
784 properties of quercetin and quercetin dihydrate in subcritical water. J. Food Eng. 100, 208-218.

785 Steffen, Y., Gruber, C., Schewe, T., Sies, H., 2008. Mono-O-methylated flavanols and other flavonoids
786 as inhibitors of endothelial NADPH oxidase. Arch. Biochem. Biophys. 469, 209-219.

787 Sun, H., Xu, H., Yang, X., Li, N., Liu, Z., Pan, W., Yuan, Y., 2011. Formulation of a stable and high-
788 loaded quercetin injectable emulsion. Pharm. Dev. Technol. 16, 609-615.

789 Teng, J., Bates, S., Engers, D.A., Leach, K., Schields, P., Yang, Y., 2010. Effect of water vapor
790 sorption on local structure of Poly(vinylpyrrolidone). J. Pharm. Sci. 99, 3815-3825.

791 Tihanyi, K., Vastag, M., 2011. Solubility, delivery and ADME problems of drugs and drug-candidates,
792 Bentham Science Publishers, Budapest.

793 Tran, T.H., Guo, Y., Song, D., Bruno, R.S., Lu, X., 2014. Quercetin- containing self- nanoemulsifying
794 drug delivery system for improving oral bioavailability. J. Pharm. Sci. 103, 840-852.

795 Trendafilova, I., Szegedi, A., Mihály, J., Momekov, G., Lihareva, N., Popova, M., 2017. Preparation of
796 efficient quercetin delivery system on Zn-modified mesoporous SBA-15 silica carrier. Mat. Sci. Eng.
797 C-Mater. 73, 285-292.

798 Vasconcelos, T., Sarmento, B., Costa, P., 2007. Solid dispersions as strategy to improve oral
799 bioavailability of poor water soluble drugs. Drug Discov. Today. 12, 1068-1075.

800 Vidanapathirana, A.K., Thompson, L.C., Mann, E.E., Odom, J.T., Holland, N.A., Sumner, S. J., Han,
801 L., Lewin, A.H., Fennell, T.R., Brown, J.M., Wingard, C. J., 2014. PVP formulated fullerene (C60)
802 increases Rho-kinase dependent vascular tissue contractility in pregnant Sprague Dawley rats. Reprod.
803 Toxicol. 49, 86-100.

804 Wang, W., 2015. Tolerability of hypertonic injectables. Int. J. Pharm. 490, 308-315.

805 Wang, W., Sun, C., Mao, L., Ma, P., Liu, F., Yang, J., Gao, Y., 2016. The biological activities,
806 chemical stability, metabolism and delivery systems of quercetin: A review. Trends Food. Sci. Technol.
807 56, 21-38.

808 Yan, J., Wu, Y.H., Yu, D.G., Williams, G.R., Huang, S.M., Tao, W., Sun, J.Y., 2014. Electrospun
809 acid–base pair solid dispersions of quercetin. RSC Adv. 4, 58265-58271.

810 Yang, L., Li, P., Gao, Y., Wu, D., 2010. Qualitative observation of chemical change rate for quercetin
811 in basic medium characterized by time resolved UV–VIS spectroscopy. J. Mol. Liq. 151, 134-137.

812 Yuan, Z.P., Chen, L.J., Fan, L.Y., Tang, M.H., Yang, G.L., Yang, H.S., Du, X.B., Wang, G.Q., Yao,
813 W.X., Zhao, Q.M., Ye, B., Wang, R., Diao, P., Zhang, W., Wu, H.B., Zhao, X., Wei, Y.Q., 2006.
814 Liposomal quercetin efficiently suppresses growth of solid tumors in murine models. Clin. Cancer Res.
815 12, 3193-3199.

816 Zhang, X., Sun, N., Wu, B., Lu, Y., Guan, T., Wu, W., 2008. Physical characterization of
817 lansoprazole/PVP solid dispersion prepared by fluid-bed coating technique. Powder Technol. 182, 480-
818 485.

819

820

821

FIGURE CAPTIONS

Figure 1. Water solubility of quercetin in solid dispersions compared to pure untreated quercetin.

Figure 2. XRPD patterns of quercetin (QCT), PVP10, and solid dispersions D12L and D12E.

Figure 3. TG and DTA curves of quercetin (QCT), PVP10, and solid dispersions D12L and D12E.

Figure 4. FT-IR spectra of quercetin, PVP10, D12M (a physical mixture of drug and polymer) and solid dispersions D12E and D12L.

Figure 5. **Changes in arterial blood pressure. A**: maximal decrease in blood pressure between pure polymer PVP10 and D12L, **B**: differences in maximal decrease in systolic and diastolic blood pressure in D12L (quercetin) treated rats. The experiments were performed on normotensive anesthetized rats.

Figure 6. Effect of D12L and PVP10 i.v. administration on arterial blood pressure in non-anesthetized spontaneously hypertensive rats. D12L was administered in the dose of 65 $mg.kg^{-1}$ corresponding to the dose of 5 $mg.kg^{-1}$ of pure quercetin. The dose of PVP10 was 60 $mg.kg^{-1}$ (this dose corresponds to the amount of PVP10 administered during the D12L application). * $p< 0.05$, ** $p< 0.01$

Figure 7. Pharmacokinetics of D12L. The graphs are showing plasma levels of quercetin and its metabolites after i.v. administration of D12L. The administered dose of quercetin was 5 mg kg^{-1}.

Figure1

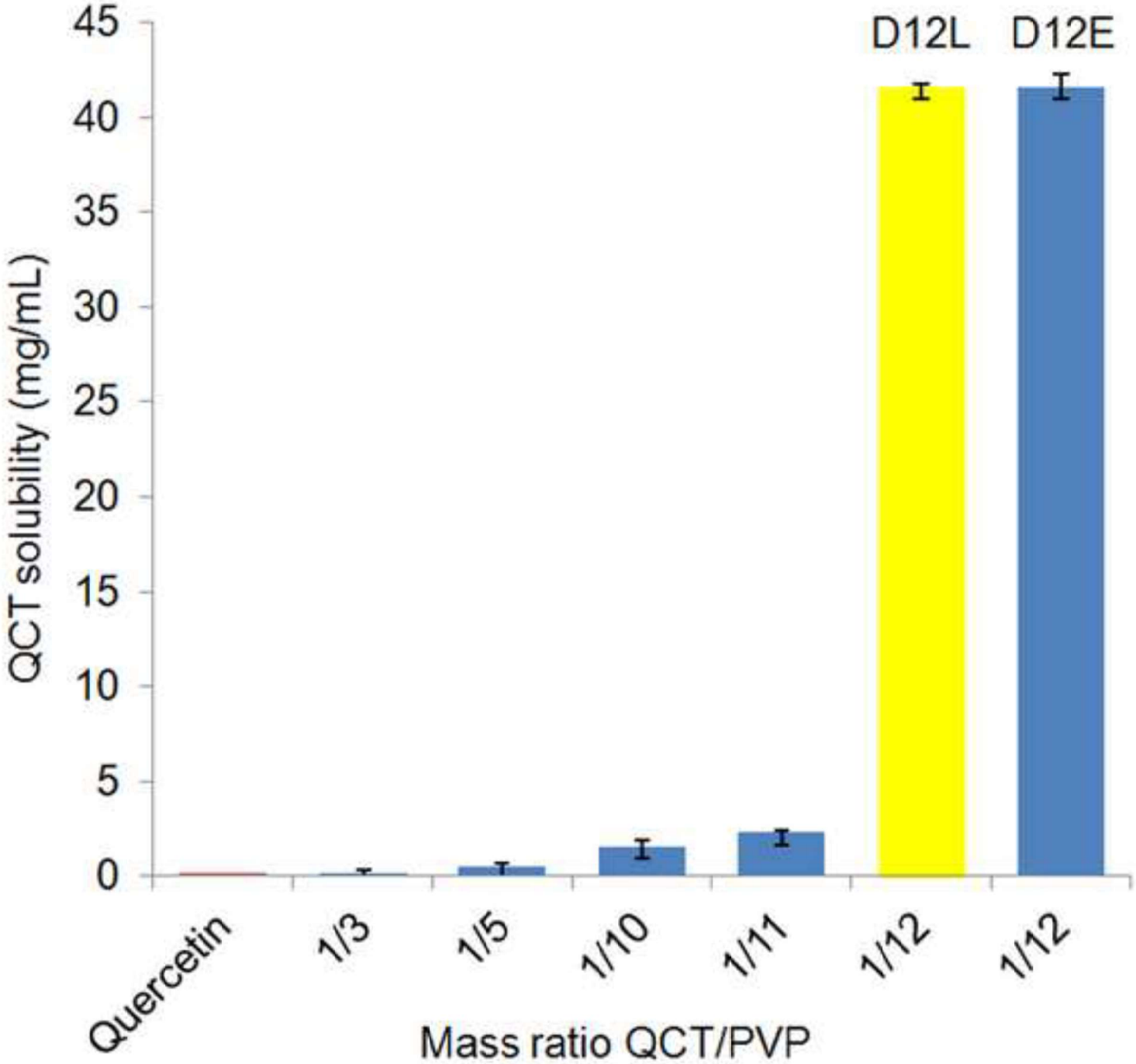
45
40
35
30
25
20
15
10
5
0
QCT solubility (mg/mL)
D12L
D12E
Quercetin
1/3
1/5
1/10
1/11
1/12
1/12
Mass ratio QCT/PVP

Figure2

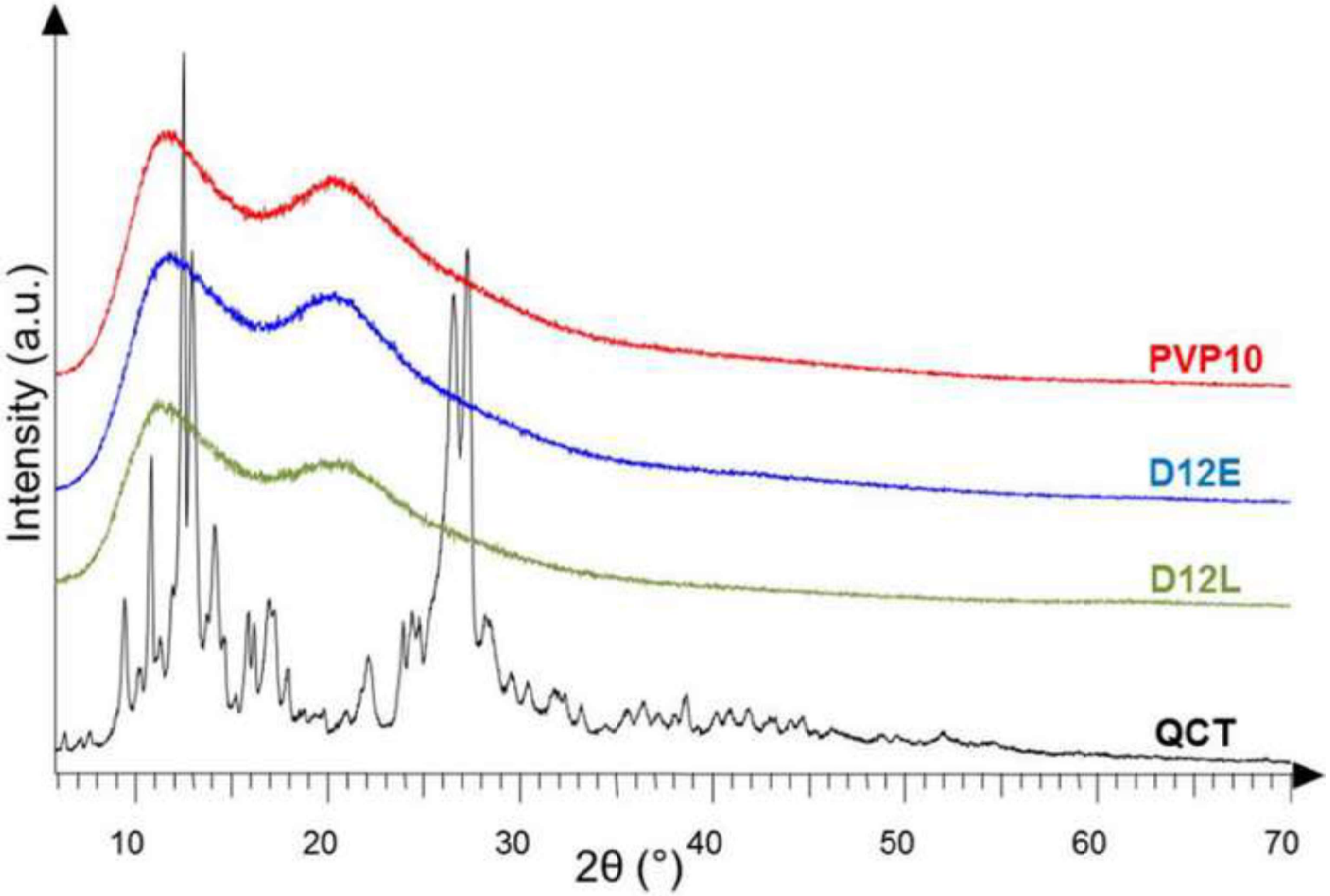

Figure3

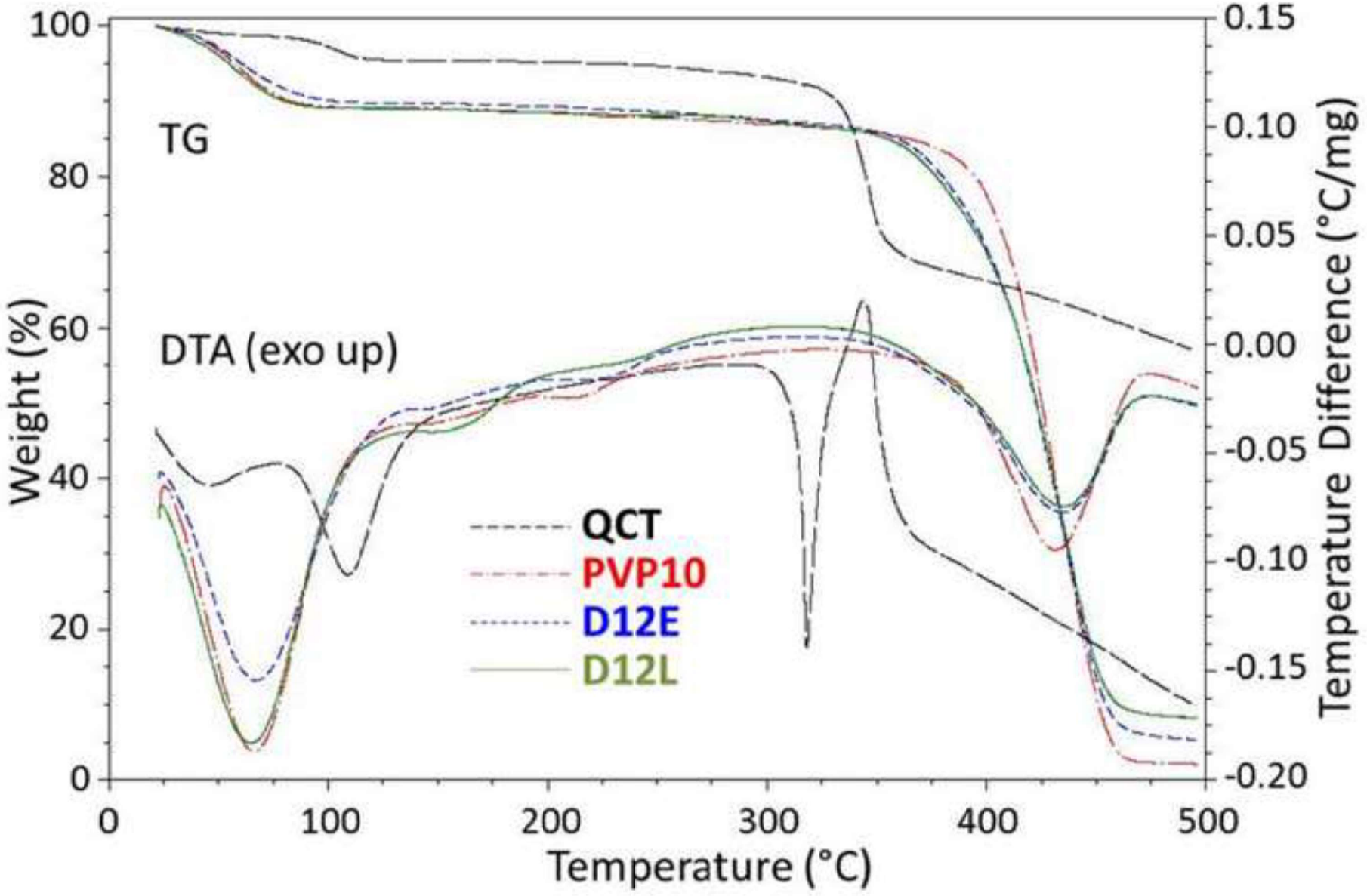
TG
DTA (exo up)
QCT
PVP10
D12E
D12L
Weight (%)
Temperature Difference (°C/mg)
Temperature (°C)
100
80
60
40
20
0
0.15
0.10
0.05
0.00
-0.05
-0.10
-0.15
-0.20
0
100
200
300
400
500

Figure4

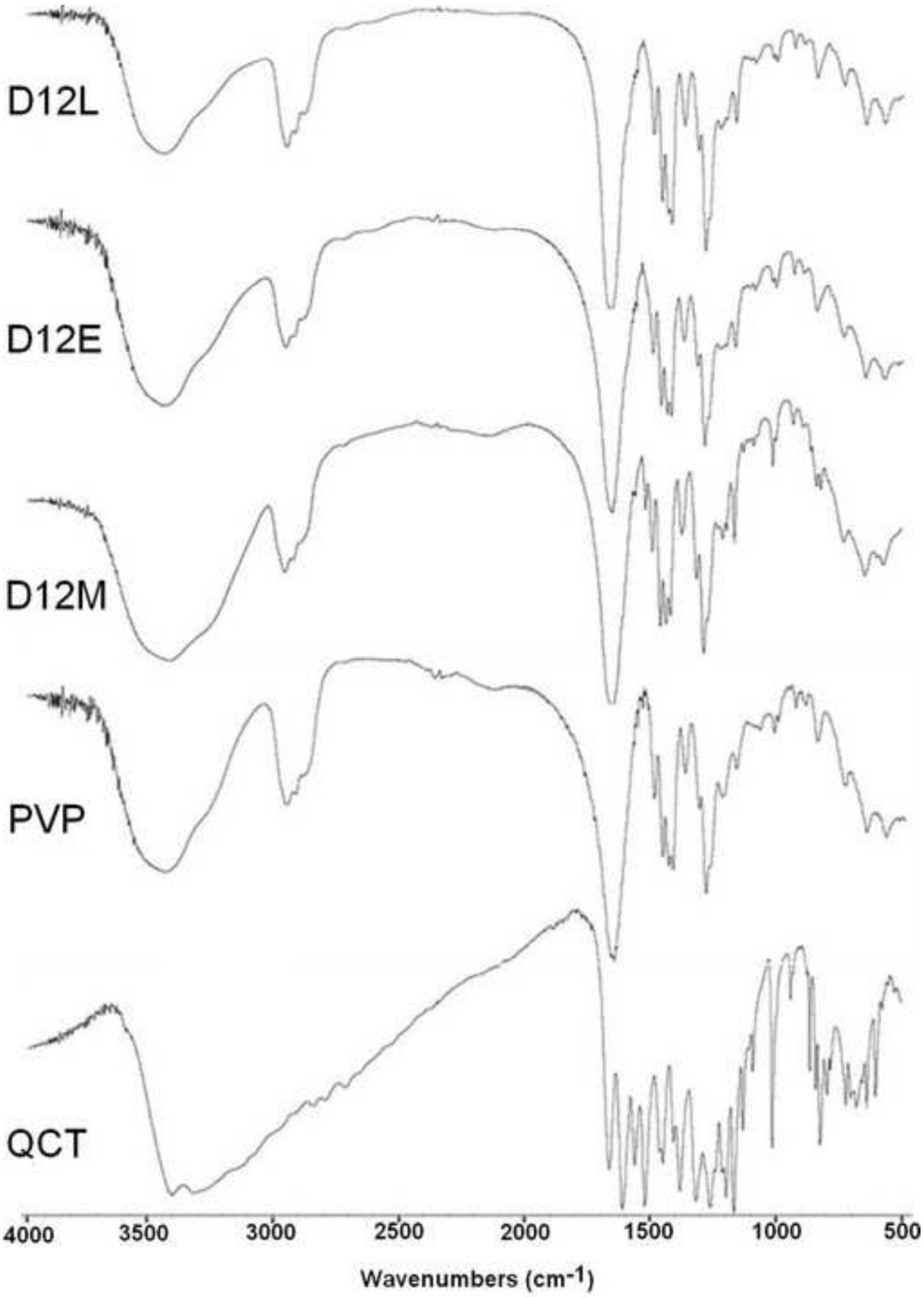
D12L
D12E
D12M
PVP
QCT
4000
3500
3000
2500
2000
1500
1000
500
Wavenumbers (cm-1)

Figure5

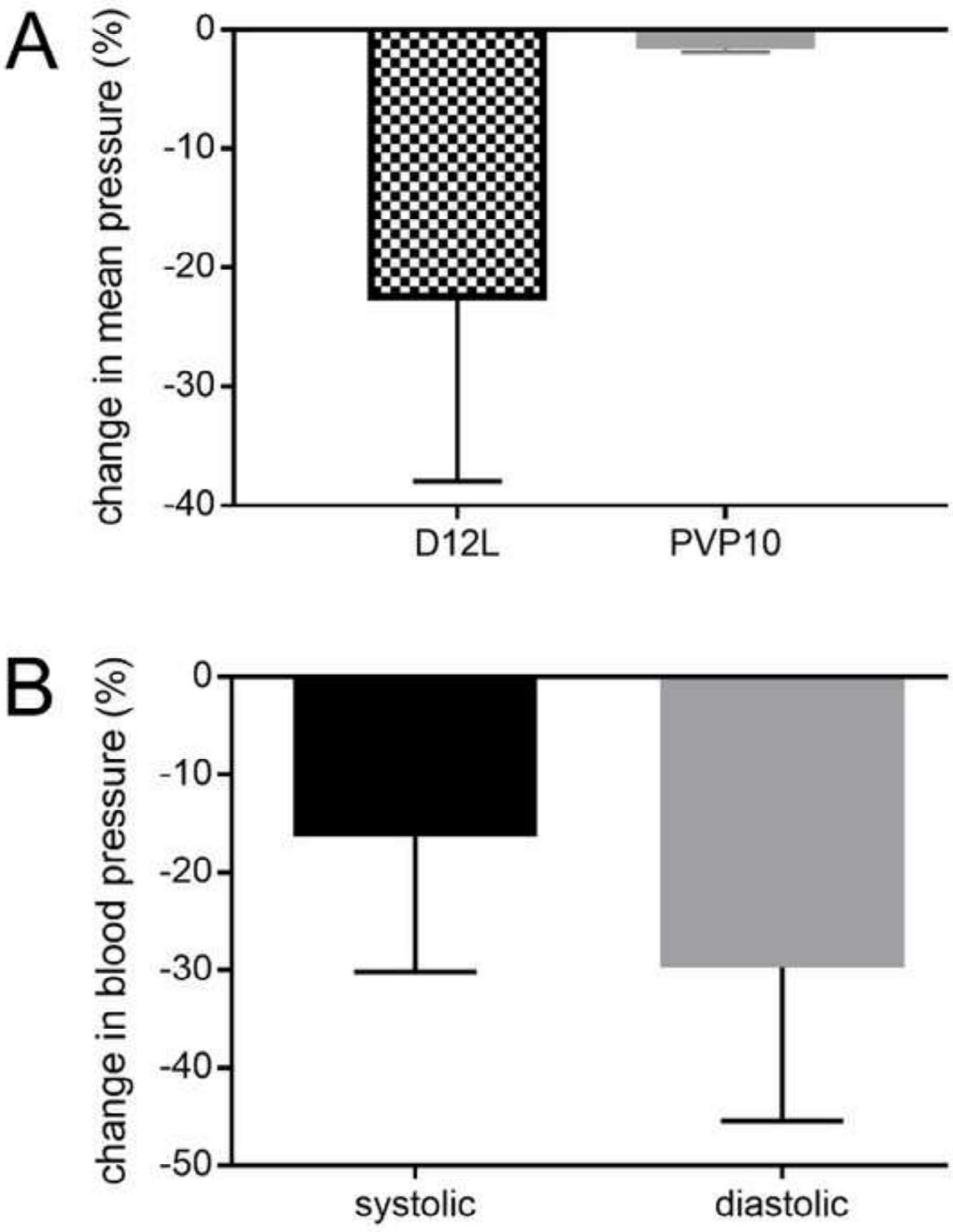
A
change in mean pressure (%)
0
-10
-20
-30
-40
D12L
PVP10
B
change in blood pressure (%)
0
-10
-20
-30
-40
-50
systolic
diastolic

Figure6

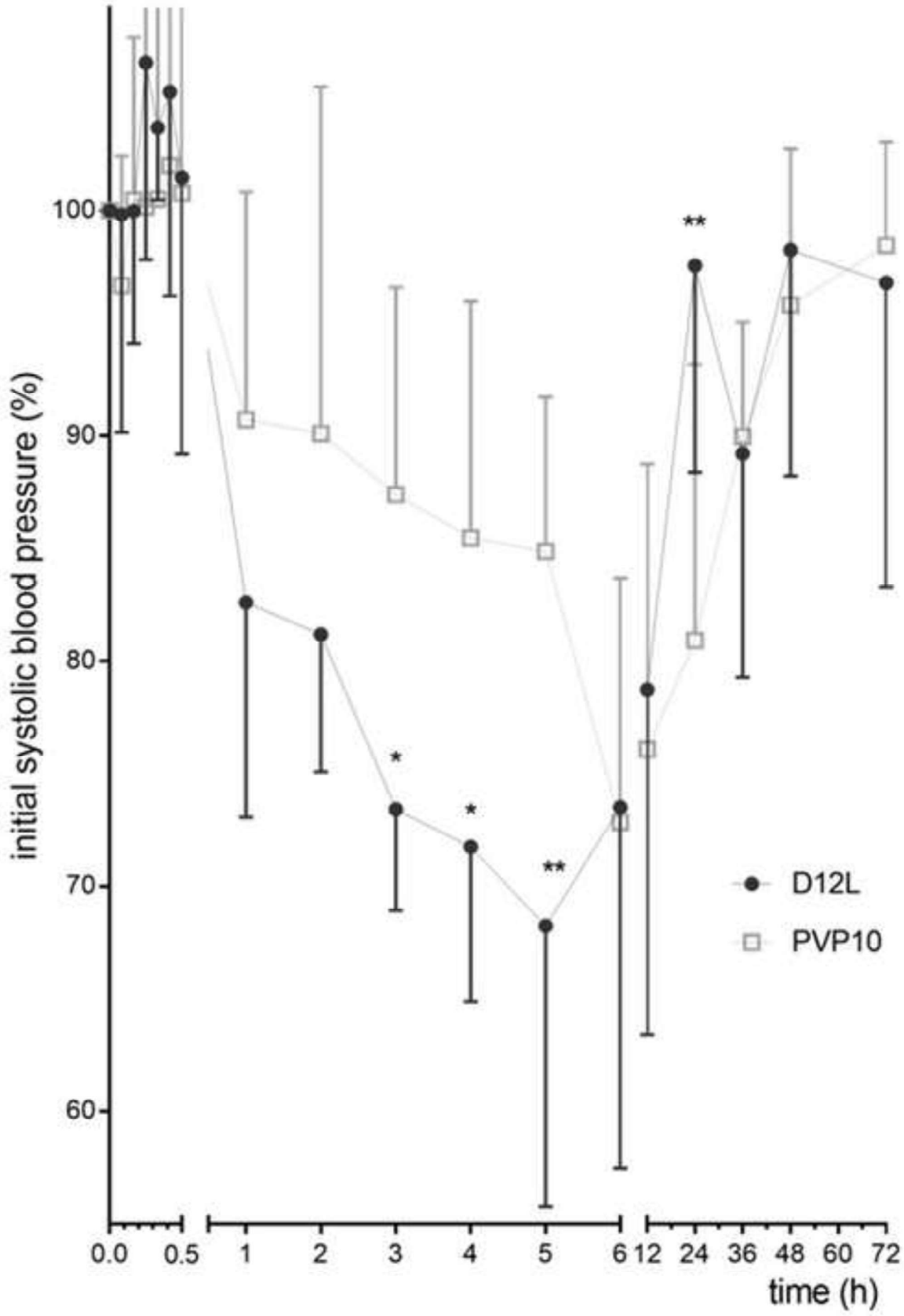
initial systolic blood pressure (%)
100
90
80
70
60
*
*
**
**
D12L
PVP10
0.0
0.5
1
2
3
4
5
6
12
24
36
48
60
72
time (h)

Figure7

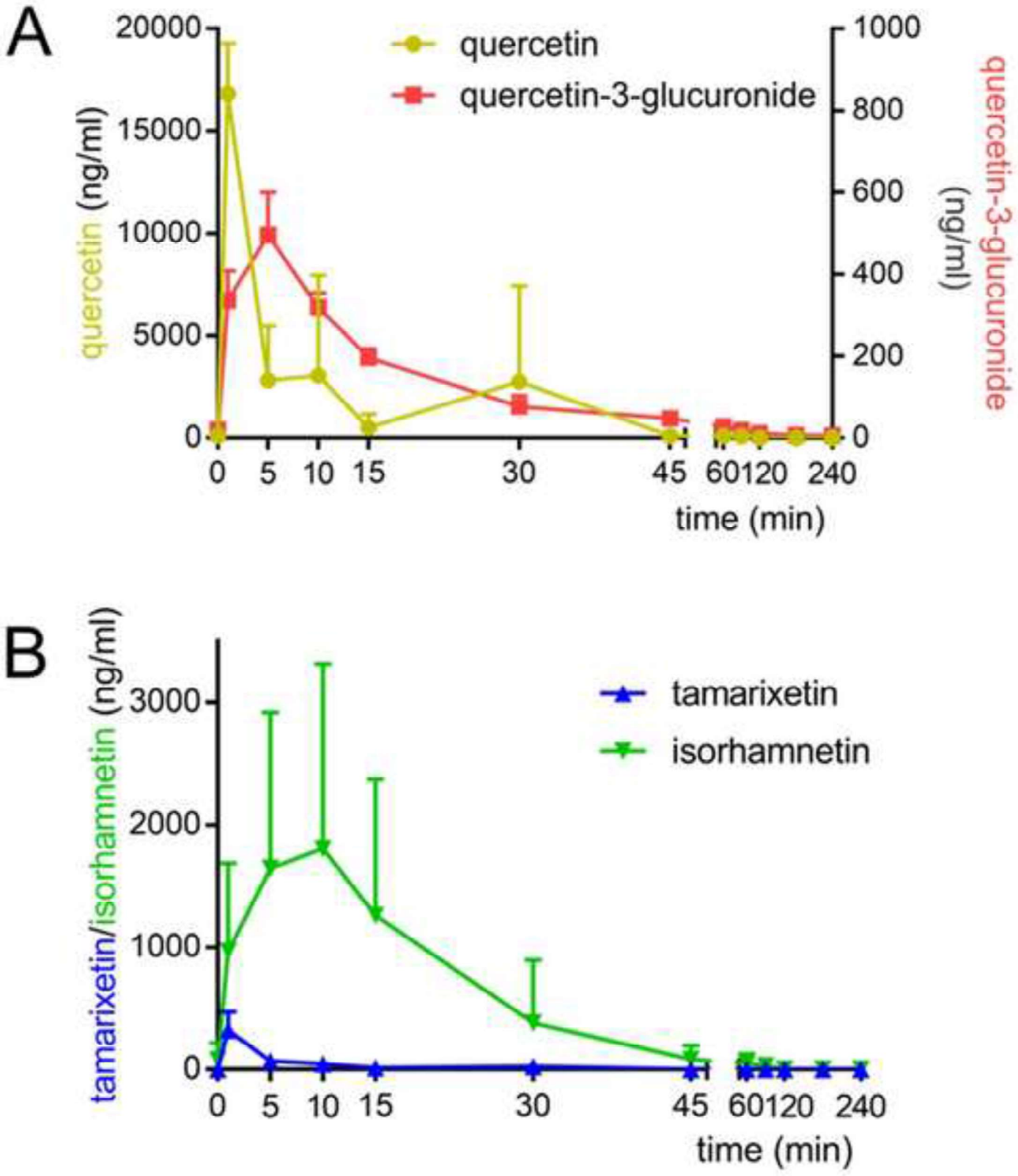
A
quercetin
quercetin-3-glucuronide
quercetin (ng/ml)
quercetin-3-glucuronide (ng/ml)
20000
15000
10000
5000
0
1000
800
600
400
200
0
0 5 10 15 30 45 60120 240
time (min)
B
tamarixetin
isorhamnetin
tamarixetin/isorhamnetin (ng/ml)
3000
2000
1000
0
0 5 10 15 30 45 60120 240
time (min)